Desalination and Water Treatment
www.deswater.com

doi: 10.1080/19443994.2015.1137497

57 (2016) 23951–23964
October

Taylor & Francis
Taylor & Francis Group

Removal of Cr(VI) from aqueous solution using *Strychnos nux-vomica* shell as an adsorbent

E. Nakkeeran, S. Rangabhashiyam, M.S. Giri Nandagopal, N. Selvaraju*

Department of Chemical Engineering, National Institute of Technology Calicut, Kozhikode 673601, Kerala, India, emails: keeran2007@gmail.com (E. Nakkeeran), rambhashiyam@gmail.com (S. Rangabhashiyam), m.s.girinandagopal@gmail.com (M.S. Giri Nandagopal), Tel. +91 495 2285409; Fax: +91 495 2287250; email: selvaraju@nitc.ac.in (N. Selvaraju)

Received 10 July 2015; Accepted 26 December 2015

ABSTRACT

In the present study, the removal of Cr(VI) from aqueous solution by a *Strychnos nux-vomica* shell was examined in a batch study. The main process parameters such as adsorbent dose, pH, initial concentration, temperature, agitation speed and contact time were studied. The result shows that the maximum removal of Cr(VI) was observed at pH 2. The progressive changes on surface texture and the confirmation of chromium binding on adsorbent surface at different stages were obtained by the scanning electron microscopy, energy-dispersive X-ray spectroscopy and Fourier transform infrared spectrometer analysis. The equilibrium data from the biosorption study was evaluated by the use of two parameter isotherm models. Langmuir isotherm model seems to fit better with the equilibrium data. Kinetic studies were performed using pseudo-first-order, pseudo-second-order and intraparticle diffusion models. The biosorption data were found to best fitted for pseudo-second-order kinetic model. The calculated thermodynamic parameters such as ΔG°, ΔH° and ΔS° showed that the adsorption of Cr(VI) ions onto adsorbents was spontaneous, endothermic and increased randomness in nature. The results indicate that STFS can be an effective adsorbent for the removal of Cr(VI) from aqueous solutions.

Keywords: Adsorption; Hexavalent chromium; *Strychnine* tree fruit shell; FTIR; Biosorption; Kinetics; Isotherms

1. Introduction

Contamination of water by toxic heavy metals is a worldwide environmental problem. Removal of heavy metals from water is essential to meet the water quality standards strictly with environmental protection laws. Amongst the heavy metals, chromium has major impact on environment amongst the above heavy metals, which has both properties that causes harmful as well as advantageous things to the environment. Some of the other heavy metals that are familiar are cadmium, chromium, cobalt, copper, lead [1], nickel, mercury [1] and zinc. Normally, chromium exists in six oxidation states. Its two most stable states are trivalent chromium (Cr^{3+}, $Cr(OH)^{2+}$) and hexavalent chromium ($HCrO_4^-$, $Cr_2O_7^{2-}$). Most of the hexavalent compounds are toxic, carcinogenic and mutagenic [2,3]. The permissible chromium concentrations in effluent discharges, as specified by the Central Pollution Control Board are 0.05 mg/L for drinking

*Corresponding author.

1944-3994/1944-3986 © 2016 Balaban Desalination Publications. All rights reserved.

water, 0.1 mg/L for inland surface water and various industries, 2 mg/L for public sewers and 1 mg/L for marine coastal areas [4]. Breathing in high levels (>2 mg/L) of chromium causes irritation to the nose such as runny nose, sneezing, itching, ulcers, etc. Long-term exposure to chromium causes lung cancer and high levels of chromium cause asthma attacks. Chromium enters aqueous waste streams from many industries such as electroplating, leather tanning, dyeing, cement, metal processing, paints and pigments, textile, wood and steel, etc. The above industries produce large quantities of toxic metal wastewater effluents. Various processes are used to remove hexavalent chromium from water and wastewater. Some of them are reverse osmosis, electrodialysis, solvent extraction, ion exchange, sulphide precipitation, chemical precipitation, electrochemical reduction, adsorption, etc. [5]. Most of these methods require high cost to implement which is not practically possible under large scale treatment. But adsorption is an economic and cost-effective method. Some of the reasons to choose adsorption process are usage of cheaper adsorbents, high process flexibility in design and operation, reusability of the adsorbents, etc. [6]. Requirements of good water quality and matters of financial constraints are encouraging the researchers and environmentalists to find suitable adsorbents. A number of studies have been reported using different kind of adsorbents for the removal of hexavalent chromium from aqueous solutions. They include tamarind seeds [7], rice bran [8]. Coir pith [9], Bael fruit shell [10], riverbed sand [11], *Erythrina variegata orientalis* leaf powder [12], lignocellulosic solid wastes [13], dry *Araucaria* leaves [14], mangrove leaf powder [15], *Salvinia cucullata* [16], barks of *Acacia albida* and leaves of *Euclea schimperi* [17], *Ficus carica* [18], neem leaf powder [19], *Peganum harmala* [20], sunflower stem waste [21], *Chrysophyllum albidum* [22], *Parthenium hysterophorus* weed [23], etc. In the present study, adsorption behaviour of Cr(VI) by strychnine tree fruit shell is studied.

2. Materials and methods

2.1. Preparation of adsorbent

Fruit shells from S*trychnine* tree (STFS) were collected from NIT Calicut campus. It was washed with tap water first and then with distilled water to remove impurities and surface sticky particles. The washed shells are then dried under natural sunlight for 7 d and then at 80˚C in a hot air oven for 2–3 d. Then it is crushed using pulverized and sieved in the size range of 0.15–.075 mm. The sieved product is again washed with distilled water for further colour removal and then it is dried at 80˚C for 1 d. It is then stored in a closed container for further use.

2.2. Preparation of synthetic sample

A stock solution of 1,000 mg/L concentration of chromium(VI) solution was prepared by dissolving the required quantity of AR grade potassium dichromate(K_2Cr_2O7) (Merck India Ltd) in 1,000 ml of distilled water. The stock solution was further diluted with distilled water to the required concentration for obtaining the test solutions. The initial metal ion concentrations ranging from 50, 100, 150, 200 and 250 mg/L were prepared.

2.3. Characterization of biosorbent

The percentage of elements C, H, N and S in the STFS was analysed using C-H-N-S Analyser (Vario EL III, Elementar, Germany). Surface area of the STFS was determined using Surface area analyser (ASAP 2200, Micromeritics, USA). The surface morphologies of the STFS before and after Cr(VI) biosorption was visualized using scanning electron microscope (SEM) (JSM – 6390LV, JEOL, USA). The Cr(VI) upload on the STFS was further confirmed by energy-dispersive X-ray spectroscopy (EDS) (JED–2300, JEOL, USA). Fourier transform infrared spectroscopy (FT-IR) spectra of STFS before and after Cr(VI) biosorption were collected in 500–4,000/cm using FT-IR spectrophotometer (Nicolet Avatar 370, Thermo Scientific, India).

2.4. Batch adsorption experiments

Batch experiments were carried out using a series of 250 ml conical flasks to investigate the effects of contact time (10, 20, 30, 40, 50, 60, 70, 80, 90, 100, 110 and 120 min), initial metal ion concentration (50, 100, 150, 200 and 250 mg/L), pH (2, 3, 4, 5, 6, 7, 8, 9), agitation speed (60, 80, 100, 120, 140, 160 rpm), temperature (303, 313, 323 and 303 K) and adsorbent dosage (0.02, 0.04, 0.06, 0.08 and 0.1 g). Known amount of adsorbents (0.08 g) were added to the solution. The pH of the solution was adjusted to required value by adding 0.1 M HCl or 0.1MNaOH using pH metre (VSI electronics Pvt. Ltd, VSI-02). Experiments were carried out at normal temperature (30˚C). The agitation of the solution was provided by a thermo stated shaking incubator (116736 GB; GeNei, India). The suspensions were filtered using Whatman filter paper no. 1 and the final chromium concentration in the filtrate was determined using a double-beam UV–visible spectrophotometer (2201, Systronics). Chromium(VI) ions

were analysed after the formation of a pink-coloured complex with 1,5 diphenylcarbazide in the acidic condition [24]. The absorbance of this coloured complex was measured at 540 nm [25]. The concentration of the analyte was determined from the calibration curve of the standards. The Chromium(VI) removal (%) at any instant of time was determined by the following equation:

$$\text{Chromium removal}\,(\%) = \frac{C_0 - C_e}{C_0} \times 100 \quad (1)$$

where C_0 and C_e are the concentrations of Cr(VI) ions initially and at a given instant of time.

The amount of Cr(VI) adsorbed (q_e) in mg/g was calculated using the following equation:

$$q_e = \frac{C_0 - C_e}{m} \times V \quad (2)$$

where C_0 and C_e are the initial and the equilibrium Cr (VI) in the aqueous solution, respectively (mg/L), m is the mass of adsorbent used (g), and V is the volume of the Cr(VI) solution (L).

3. Results and discussions

3.1. Characterization of biosorbent

The chemical and physical characteristics of STFS were presented in Table 1. scanning electron microscopy (SEM) technique was used to examine the surface physical morphology of the adsorbent.

Fig. 1(a) and (b) illustrate the SEM images of STFS in raw form and Cr(VI)-loaded STFS, respectively. Significant differences were observed between the two figures in the surface physical arrangement of STFS. As shown in Fig. 1(a), the surface of STFS is moderately smooth and porous structures are not noticed anywhere on it. In Fig. 1(b), some cavities can be observed and some pores of various shapes and sizes were observed which can leads to an increase in adsorption properties of Cr(VI) of STFS.

Table 1
Physical and Chemical properties of STFS used in the experiments

Parameter	Value
Elemental analysis (%)	
C	44.75
H	5.66
N	0.79
Surface area	3.3266 m^3/g
Particle size	0.15–0.75 mm
Pore volume	0.017026 cm^3/g
Conductivity	2.823 mS/cm

The EDX spectra of the STFS before and after Cr(VI) adsorption are shown in Fig. 2. Chromium-loaded adsorbents showed distinct peaks of Cr(VI) ions present on the adsorbent surface Fig. 2(b). Therefore, EDX analysis confirmed the adsorption of Cr(VI) onto STFS.

The FTIR spectra of STFS before and after chromium adsorption were observed to collect the information regarding changes in wave number on the functional groups in the range of 500–4,000 cm^{-1} (Figs. 3a and 3b). The band frequency around 3,378.58 indicates the hydroxyl groups exist there, and the reasonable shift from 3,378.58 to 3,374.05 cm^{-1} indicates that the hydroxyl groups binded with chromium. The band 2,924.91 and 2,920.16 cm^{-1} are assigned to stretching vibrations of the C–H groups. The peak observed at 1,728 and 1,662 cm^{-1} corresponds to the C=O stretching and C=C stretching, respectively. The band 1,427.47 and 1,456.94 cm^{-1} are the stretching vibrations of methoxy groups (–OCH_3) from the lignin structure of STFS can be observed [26,27]. In the region between 1,043.22 and 1,051.58 cm^{-1}, the peaks observed indicates C–O, C–OH stretching. Between the regions 1,043.22 and 606.46 cm^{-1}, 1,051.58 and 613.45 cm^{-1}, the observed peaks indicates the –C–C– and –CN stretching [28,29].

3.2. Effect of agitation speed

Biosorption of Cr(VI) on STFS was carried out by varying agitation speed at 2 pH and 90 min of contact time. Fig. 4 illustrates that the amount of Cr(VI) biosorption increases with increase in agitation speed up to 100 rpm and if the agitation speed increases further, biosorption capacity decreases. At low agitation speed, biosorbent gets accumulated at bottom portion, resulted in less exposure of various active sites and thereby have comparatively less Cr(VI) uptake. But the higher agitation speed lowers the biosorption capacity due to insufficient contact time of STFS to uptake the Cr(VI) ions [30]. An optimum agitation speed of 100 rpm was selected for the batch biosorption experiments based on the results obtained.

3.3. Effect of STFS dosage

Cr(VI) removal was studied by varying the STFS dosage in 50 mL of 50 mg/L initial Cr(VI) concentration, temperature (303 K), pH (2.0) and agitation speed

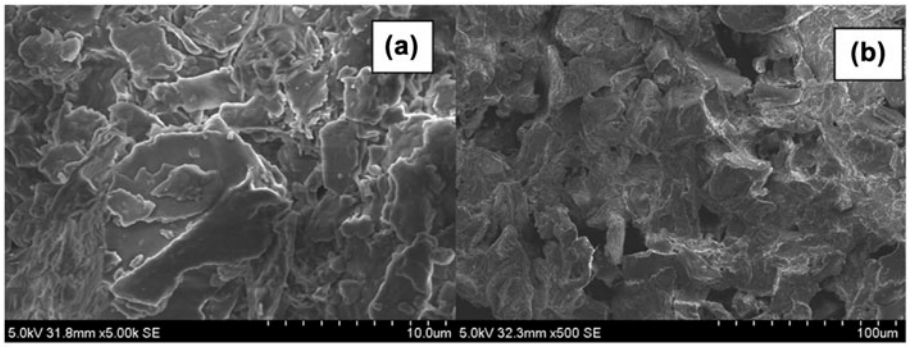

Fig. 1. Scanning electron micrographs of STFS (a) before adsorption and (b) after adsorption.

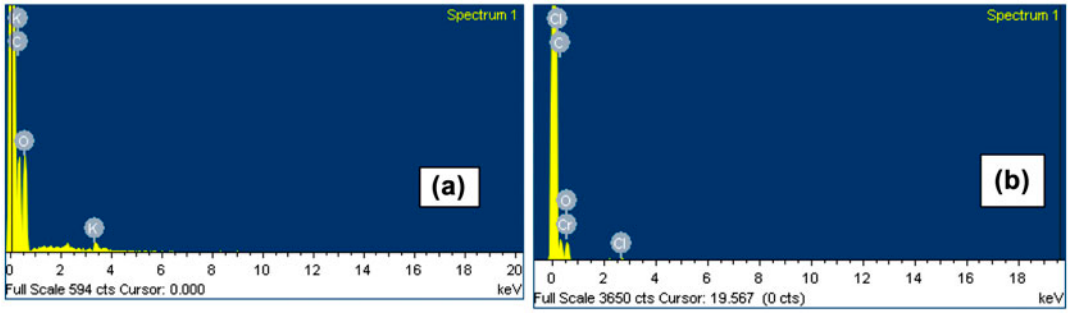

Fig. 2. EDX spectra image of STFS (a) before Cr(VI) adsorption and (b) after Cr(VI) adsorption.

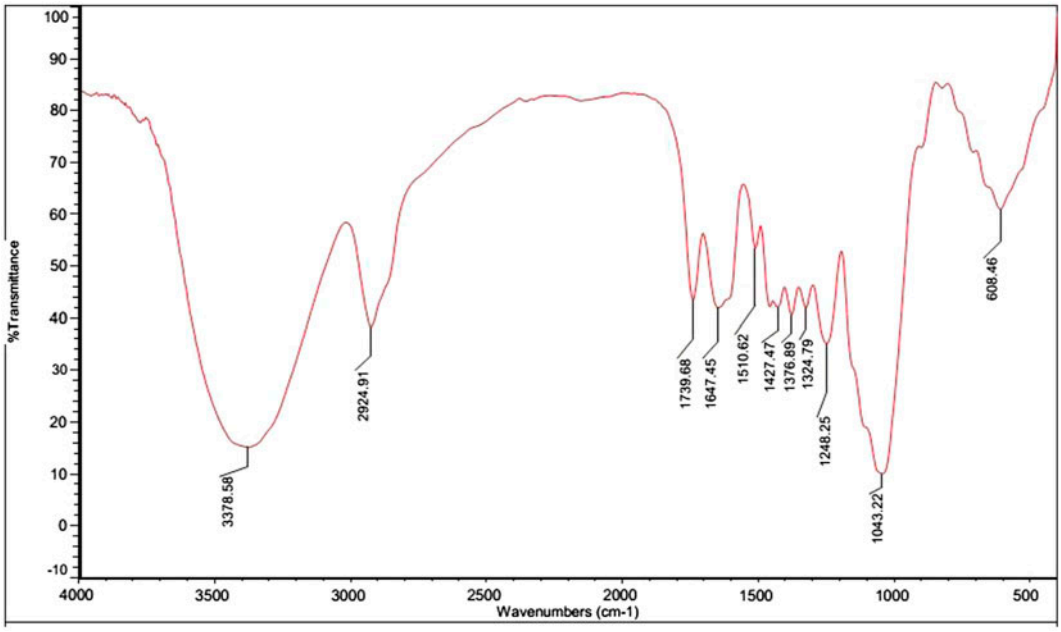

Fig. 3a. FTIR spectra image of STFS before adsorption.

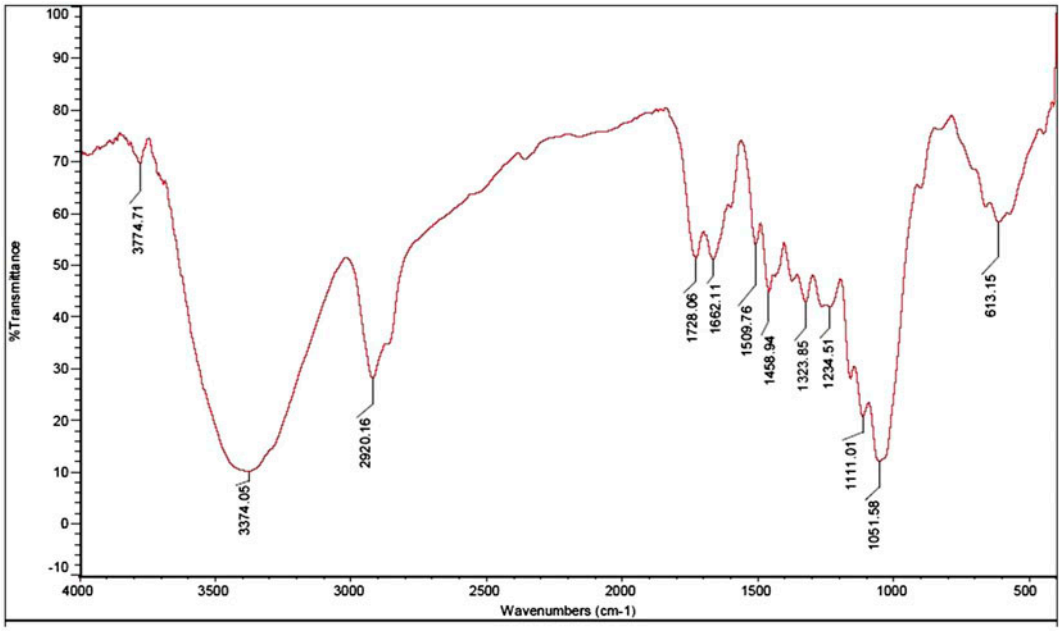

Fig. 3b. FTIR spectra image of STFS after adsorption.

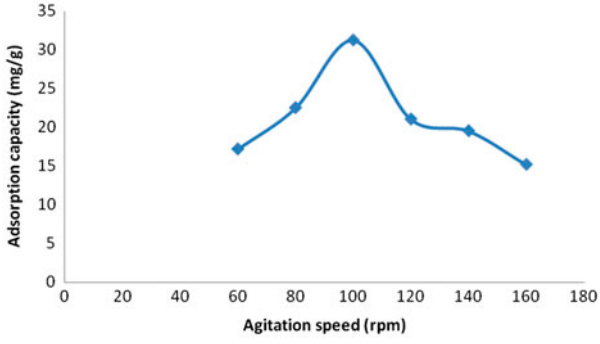

Fig. 4. Effect of agitation speed in biosorption capacity of STFS.
Notes: Conditions: amount of STFS 0.08 g, pH 2, Cr(VI) concentration 50 mg/L, temperature 303 K.

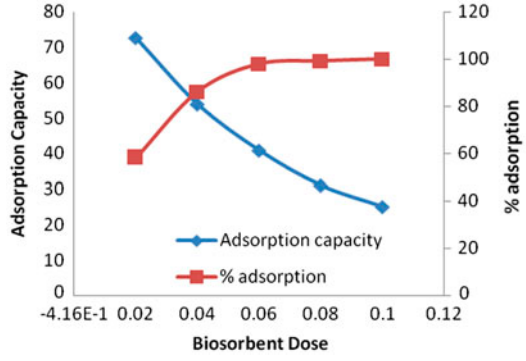

Fig. 5. Effect of biosorbent dose on Cr(VI) percentage adsorption and adsorption capacity of STFS.
Notes: Conditions: pH 2, Cr(VI) concentration 50 mg/L, agitation speed 100 rpm, temperature 303 K.

(100 rpm) constant for 90 min. The Cr(VI) uptake capacity of the STFS was found to have decreased from 72.625 mg/g at low biosorbent dosage (0.02 g/L) to 25 mg/g at high biosorbent dosage (0.1 g/L) as shown in Fig. 5. At the same time, the percentage biosorption increases from 58.09% at low dosage (0.02 g/L) to 100% at higher dosage (0.1 g/L) which is shown in Fig. 5. This trend is more common because the number of active sites available in the biosorbent for the removal of Cr(VI) will be more for the increase in adsorbent dose and will be less for low dose. This is due to the reason of progressive saturation of active sites. Such type of results have also been reported in the biosorption of Cr(VI) using carbonaceous adsorbents prepared from waste biomass [31].

3.4. Effect of pH

One of the important parameters for the adsorption process is pH as it controls the adsorption capacity due to its influence on the surface properties of adsorbent and ionic forms of metal ions in the solution. Batch adsorption experiments were conducted by varying the pH from 2.0 to 9.0 in 50 ml of 50 mg/L of initial Cr(VI) concentration, adsorbent dose (0.08 g),

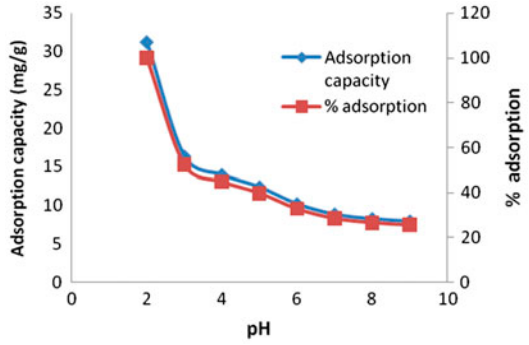

Fig. 6. Effect of pH on Cr(VI) percentage adsorption and Adsorption capacity by STFS.
Notes: Conditions: amount of STFS 0.08 g, Cr(VI) concentration 50 mg/L, agitation speed 100 rpm, temperature 303 K.

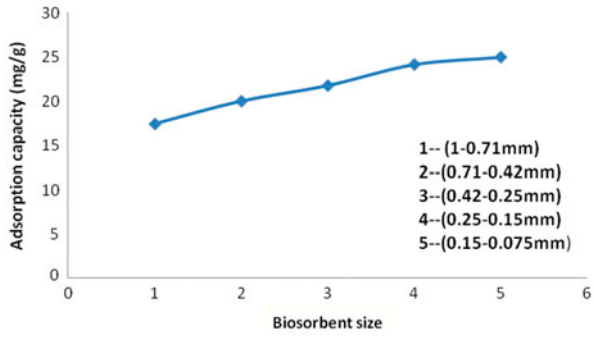

Fig. 7. Effect of biosorbent size on adsorption capacity by STFS.
Notes: Conditions: 90 min contact time, 2 pH and 0.1 g of STFS.

temperature(303 K), agitation speed (100 rpm) and for time (90 min). As shown in Fig. 6, the adsorption capacity was found to be maximum at pH 2.0 which is around 31.14 mg/g. Also the percentage biosorption was found to be maximum at the same pH and it was 99.66%. It was also observed that as pH increases further, there is a decline in percentage biosorption and adsorption capacity. These observations can be obtained based on the reasons such as: (i) the pH of the aqueous solution affects the Cr(VI) ion speciation and (ii) at lower pH, the adsorbent surface is positively charged that results in strong electrostatic attraction between positively charged adsorbent surface and negatively charged chromate ions [21]. As the pH increased, the overall surface charge on the adsorbents became negative and adsorption gets decreased. As Cr (VI) removal was found to be maximum at pH 2.0, it was taken as the optimal pH value for further adsorption experiments [32].

3.5. Effect of biosorbent size

The effect of biosorbent size for the removal of Cr(VI) and adsorption capacity at 90 min contact time, 2 pH and 0.1 g of STFS. The results indicated that the percentage adsorption and biosorption capacity of Cr(VI) was decreased with the increase in biosorbent size. The plot between adsorption capacity and biosorbent size is shown in Fig. 7 The reason for this is improvement in surface area has increased binding sites and contact surfaces, which results in higher mass transfer and increase in biosorption. Since it is a surface phenomenon, the degree of biosorption was directly proportional to the biosorbent surface area. Therefore, if the biosorbent size is smaller, the surface area will be greater and that results in higher biosorption. Therefore, 0.015–0.075 mm size of STFS was selected for the present experimental purpose.

3.6. Effect of temperature

The effect of temperature on Cr(VI) uptake capacity of STFS for five different initial concentrations is presented in Fig. 8. It can be seen from the figure that Cr(VI) uptake decreases when the temperature increased from 30 to 60°C. The decrease in uptake capacity with increase in temperature explains the exothermic nature of the adsorption process. This observation also suggests that weak adsorption interaction between the surface of the biomass and the metal ion which favours physisorption [33,34]. Similar observations have also been reported in the biosorption of Cr(VI) from aqueous solutions by *P. hysterophorus* weed [23].

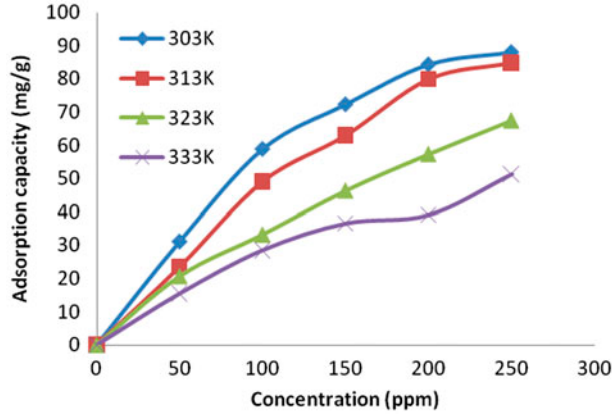

Fig. 8. Effect of temperature on adsorption capacity by STFS.
Notes: Conditions: 90 min contact time, 2 pH, agitation speed 100 rpm and 0.08 g of STFS.

3.7. Effect of initial Cr(VI) concentration and contact time

The effect of initial Cr(VI) concentration on percentage biosorption by STFS was analysed at different initial concentrations varying from 50 to 250 mg/L, at pH 2.0 and at temp. 303 K .It was observed that by increasing the Cr(VI) concentration, a decrease in percentage Cr(VI) biosorption (from 99.66 to 56.29%) results as shown in Fig. 9. The reason for this is at low Cr(VI) concentration, most of the Cr(VI) ions in the solution would react with available binding sites on the biosorbent and therefore higher biosorption results [14,35]. Also, it was observed that the adsorption capacity increases (from 31.14 to 87.95 mg/g) as the initial concentration increases, which is shown in Fig. 10.

3.8. Adsorption isotherms

To examine the mechanism of Cr(VI) adsorption onto the adsorbents, the equilibrium adsorption isotherms are very important. They are also important in the modelling and designing of adsorption systems. The equilibrium data were applied to the isotherm models like Langmuir, Freundlich, Dubinin–Radushkevich, Halsey, Flory–Huggins, Jovanovic and Temkin [36].

3.9. Langmuir model

This model provides the information on capability of adsorption and it reflects the equilibrium adsorption process behaviour. This Langmuir isotherm is based on the assumption of monolayer coverage of adsorbate over a homogeneous adsorbent surface [37]. It can be explained by the equation:

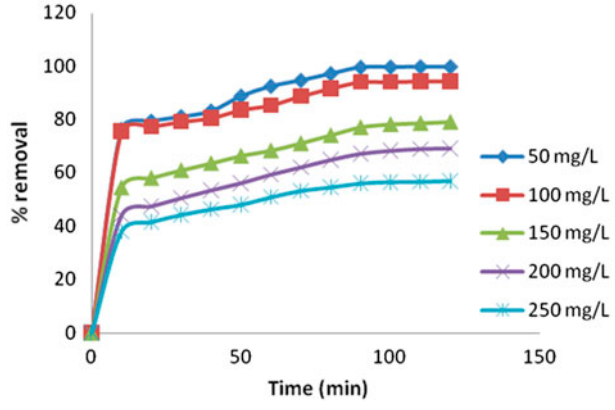

Fig. 9. Effect of contact time and initial Cr(VI) concentration on % of Cr(VI) removal by STFS.
Notes: Conditions: STFS dose 0.08 g, pH 2, temperature 303 K.

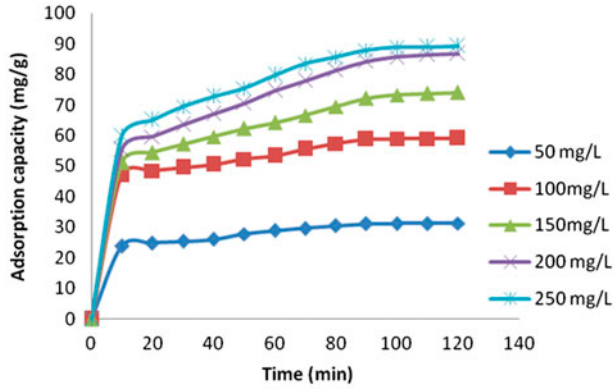

Fig. 10. Effect of contact time and initial Cr(VI) concentration on adsorption capacity by STFS.
Notes: Conditions: STFS dose 0.08 g, pH 2, temperature 303 K.

$$q_e = \frac{Q_0 b_L C_e}{1 + b_L C_e} \tag{3}$$

where C_e is the equilibrium concentration of Cr(VI) (mg/L), q_e is the amount of Cr(VI) adsorbed per gram of biosorbent at equilibrium (mg/g), Q_0 is the monolayer coverage capacity (mg/g) and b_L is the Langmuir isotherm constant (L/mg).

The Langmuir isotherm is expressed in terms of the equilibrium constant R_L, which is referred as the separation factor and is dimensionless:

$$R_L = \frac{1}{1 + b_L C_i} \tag{4}$$

where C_i is the initial concentration of Cr(VI) (mg/L). The R_L value is indicative of the nature of the adsorption; it is unfavourable if $R_L > 1$, favourable if $0 < R_L > 1$, and irreversible if $R_L = 0$.

A plot of C_e/q_e vs. C_e provides a straight line of slope $1/Q_0$ and intercepts $1/Q_0 b_L$ and is given in Fig. 11. Coefficient of determination R^2 is 0.995 and is represented in Table 2. Since R^2 value is high, this is considered as the best fit to the adsorption of Cr(VI) by this adsorbent as shown in Fig. 12. The value R_L decreases from 0.06 to 0.0136 as the initial concentration increases from 50 to 250 mg/L. The calculated values of R_L lies between 0 and 1 and that shows the adsorption of Cr(VI) is favourable under these conditions.

3.10. Freundlich model

This isotherm represents the multilayer adsorption on the surface of adsorbents [38]. The Freundlich model is represented by the empirical equation as:

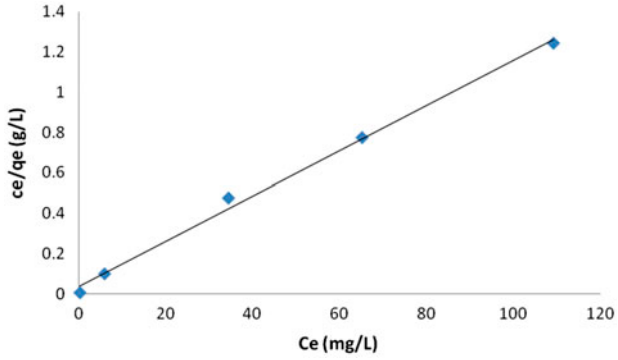

Fig. 11. Langmuir isotherm plot for the adsorption of Cr (VI) on STFS.

$$q_e = k_f C_e^{1/n} \quad (5)$$

where q_e is the amount of Cr(VI) adsorbed per gram of biosorbent at equilibrium (mg/g), C_e is the equilibrium concentration of Cr(VI) (mg/L), k_f and n are Freundlich constants that represents the adsorption capacity and intensity, respectively. A plot of $\log q_e$ vs. $\log C_e$ provides the slope and intercept by which we can calculate the Freundlich constants. The value of $1/n$ is found to be as 0.16 which is less than unity. This suggests that the adsorption of Cr(VI) is favourable for this adsorbent under these conditions. The value of R^2 is found to be as 0.993 and is represented in Table 2.

3.11. Temkin model

This model is represented by the equation:

$$q_e = \frac{RT}{b_T} \ln A_T C_e \quad (6)$$

where q_e is the amount of Cr(VI) adsorbed per gram of biosorbent at equilibrium (mg/g), C_e is the equilibrium concentration of Cr(VI) (mg/L), A_T is the Temkin isotherm equilibrium binding constant (L/mg) and b_T is the Temkin isotherm constant (J/mol). This model

Table 2
Isotherm constants of the two variable models for biosorption of Cr(VI) by STFS

Models	Variables	Values	Coefficient of determination, R^2
Langmuir	Q_o (mg/g)	90.9	
	b_L (L/mg)	0.289	0.995
R_L, for values of C_i (mg/L)			
	50	0.06	
	100	0.033	
	150	0.022	
	200	0.017	
	250	0.0136	
Freundlich	k_f (mg/g)	42.237	0.993
	n	6.25	
Dubinin–Radushkevich	Q_m (mg/g)	74.8	0.864
	K (mol^2 KJ^{-1})	2×10^{-5}	
	E (kJ/mol)	158.11	
Temkin	A_T (L/mg)	1.005	0.985
	b_T (kJ/mol)	0.2896	
Jovanovic	q_{mj} (mg/g)	45.71	0.618
	K_j (L/g)	−.002	
Halsey	K_H	6.9×10^{-11}	
	n_H	−6.25	0.994
Flory–Huggins	K_{FH}	1.03×10^{-6}	
	n_{FH}	−2.221	0.911

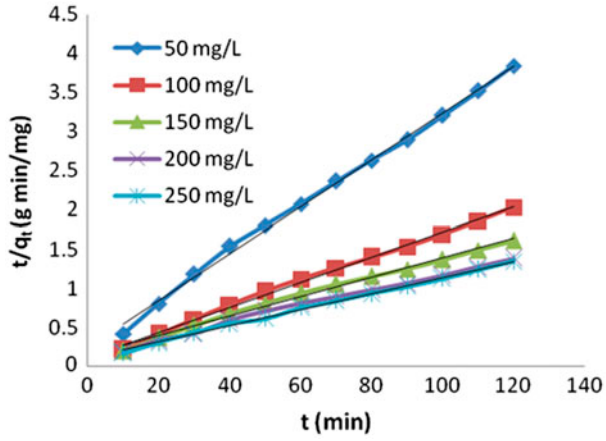

Fig. 12. Pseudo-second-order kinetic model of STFS for different initial Cr(VI) concentrations.

represents a factor of the interaction of adsorbent and adsorbate. Also it mentions a fact that the heat of adsorption of all molecules in the layer decreases linearly [39]. A plot of q_e vs. ln C_e was used to find the Temkin isotherm constants A_T and b_T, respectively, and listed in Table 2. The value of R^2 is found to be as 0.985 and is indicated in Table 2.

3.12. Jovanovic model

The equation of this model is represented as:

$$q_e = q_{mj}(1 - e^{K_j C_e}) \tag{7}$$

where q_e is the amount of Cr(VI) adsorbed per gram of biosorbent at equilibrium (mg/g), C_e is the equilibrium concentration of Cr(VI) (mg/L), q_{mj} and K_j are the maximum adsorption capacity (mg/g) and Jovanovic isotherm constant, respectively. This model represents the approximation of monolayer localized adsorption without any interactions. This model of an adsorption surface is similar to that of Langmuir isotherm model [40]. A plot of log q_e vs. C_e is used to determine the value of K_j and q_{mj} and is listed in Table 2. The value of R^2 (0.618), maximum adsorption capacity and the Jovanovic isotherm constant are found to be less when compared to the value of Langmuir isotherm model and is listed in Table 2.

3.13. Dubinin–Radushkevich model

The equation related to this model is given as:

$$q_e = Q_m \exp^{-K\varepsilon^2} \tag{8}$$

where q_e is the amount of Cr(VI) adsorbed per gram of biosorbent at equilibrium (mg/g), Q_m is the maximum adsorption capacity (mg/g), K is the coefficient related to the mean free energy of adsorption (mol^2/kJ^2), ε is the Polanyi potential which can be calculated by the equation:

$$\varepsilon = RT \ln\left(1 + \frac{1}{C_e}\right) \tag{9}$$

where R is atmospheric gas constant (8.314 J/mol K), T is the temperature (K) and C_e is the equilibrium concentration of Cr(VI) (mg/L).

The mean adsorption energy E (kJ/mol) was calculated using the following equation:

$$E = \sqrt{2K} \tag{10}$$

If this means adsorption energy is less than 8 kJ/mol, physisorption dominates. If it is greater than 16 kJ/mol, then chemisorptions dominates. If it lies between 8 and 16 kJ/mol, then it shows that the adsorption results because of ion-exchange mechanism [41]. The value of maximum adsorption capacity, mean free energy of adsorption, Polanyi potential was determined by a plot between log q_e and ε^2. The mean adsorption energy was found to be 158.11 kJ/mol which shows that chemisorption dominates here. The value of R^2 is found to be less (0.864) and is listed in the Table 2.

3.14. Halsey model

This model can be represented by the equation:

$$q_e = \exp\left(\frac{\ln K_H - \ln C_e}{n_H}\right) \tag{11}$$

where q_e is the amount of Cr(VI) adsorbed per gram of biosorbent at equilibrium (mg/g), C_e is the equilibrium concentration of Cr(VI) (mg/L). Halsey proposed this model based on the condensation of a multilayer process at a larger distance from the surface [42]. K_H and n_H are Halsey isotherm constants which can be estimated by the plot between ln q_e and ln C_e. The values of the isotherm constants and coefficient of determination R^2 are listed in Table 2. The results show that adsorption is favourable under the specified conditions.

3.15. Flory–Huggins model

This model can be expressed in the equation form as:

$$\frac{Q}{C_0} = K_{FH}(1-Q)^{n_{FH}} \tag{12}$$

where K_{FH} and n_{FH} are indication of equilibrium constant and model exponent. Here, Q is the degree of surface coverage which can be estimated by:

$$Q = 1 - \frac{C_e}{C_0} \tag{13}$$

where C_e and C_0 are the equilibrium concentration and initial concentration in mg/L, respectively. This model describes the feasibility and nature of the adsorption process [43]. It also mentions the degree of surface coverage characteristics of the adsorbate on the adsorbent. A plot of $\log(Q/C_0)$ and $\log(1-Q)$ gives the slope and intercept by which the values of K_{FH} and n_{FH} can be estimated. By the values of K_{FH} and n_{FH} and by the value of R^2, we can come to the conclusion that this model does not favour adsorption process.

3.16. Biosorption kinetics

To design the batch biosorption systems, the analysis over the biosorption kinetics is a very important one. Kinetic models like pseudo-first-order, pseudo-second-order and intraparticle diffusion models were used to fit the equilibrium data to predict the mechanism of biosorption and to find the performance of biosorbent.

3.17. Pseudo-first-order kinetics

The equation of this model is expressed as:

$$\log(q_e - q) = \log q_e - \frac{k_1}{2.303}t \tag{14}$$

where q_e and q are the amounts of Cr(VI) adsorbed (mg/g) at equilibrium time and at any time t [28]. k_1 (min) is the pseudo-first-order rate constant. The constants value of pseudo-first-order kinetics were calculated from the plot of $\log(q_e - q)$ against t and showed in Table 3. This is applicable if the rate of adsorption of a solute by the adsorbent depends on capacity of the adsorbent. The calculated q_e values seem to be not matched with the experimental values of q_e and the coefficient of determination was found in the range from 0.810 to 0.915, which were comparatively low. From the results, the pseudo-first-order model was not found suitable for modelling the biosorption of Cr (VI) onto STFS.

3.18. Pseudo-second-order kinetics

Equation related to this model is expressed as

$$\frac{t}{q_t} = \frac{1}{k_2 q_e^2} + \frac{t}{q_e} \tag{15}$$

where k_2 (g/mg/min) is the pseudo-second-order constant [44]. The constants value of pseudo-second-order kinetics was calculated from the plot of t/q_t against t which is shown in Fig. 12. From the values shown in Table 3, it seems that the biosorption of Cr(VI) onto STFS better suits this model.

3.19. Intraparticle diffusion model

This model is expressed in equation form as:

$$Q_t = k_{id}\, t^{1/2} + C \tag{16}$$

Table 3
Values of kinetic rate constants of the biosorption of Cr(VI) onto STFS

Cr(VI) Conc. (mg/L)	Pseudo-first-order			Pseudo-second-order			Intraparticle diffusion		
	$k_{1(cal)}$ (min)	q_e (mg/g)	R^2	$k_{2(cal)}$ (g/mg/min)	q_e (mg/g)	R^2	k_{id} (mg/g/min$^{1/2}$)	C	R^2
50	31.40	0.055	0.810	0.0197	33.3	0.997	1.106	19.92	0.963
100	51.88	0.052	0.841	0.0037	62.5	0.996	1.785	32.43	0.959
150	58.34	0.046	0.880	0.0011	83.3	0.994	3.231	39.96	0.988
200	95.72	0.043	0.848	0.0007	96.4	0.992	4.461	40.07	0.987
250	82.22	0.037	0.915	0.0009	98.7	0.996	4.103	47.31	0.981

Table 4
Thermodynamic parameters for the adsorption of Cr(VI) by STFS

Temperature (K)	ΔG° (kJ/mol)	ΔH° (kJ/mol)	ΔS° (kJ/molK)
303	−13.155	0.332	25
313	−1.705		
323	−1.32		
333	−0.554		

where k_{id} is the intraparticle diffusion rate constant (mg/g/min$^{1/2}$) and C is the intercept. This diffusion occurs only when q_t is a linear function of $t^{1/2}$. The constant values and the intercept values are listed in Table 3. The plot of q_t against $t^{0.5}$ shows multi-linearity correlation which informs us there exist two or more steps during biosorption process. The initial phase might be due to boundary layer diffusion [45]. The second linear portion is the gradual biosorption stage, where intraparticle diffusion is rate controlled. The increase in the C values shows that there is an increase in boundary layer thickness. It then leads to the greater contribution of the surface biosorption in the rate-controlling step.

3.20. Thermodynamic study of Cr(VI) adsorption

To illustrate the nature of removal of Cr(VI) by adsorbents, the thermodynamic parameters like change in Gibbs free energy (ΔG°), change in enthalpy (ΔH°) and change in entropy (ΔS°) will be used. These parameters were found using the following expressions:

$$\Delta G^\circ = -RT \ln k_c \tag{17}$$

$$\ln k_c = -\frac{\Delta H^\circ}{RT} + \frac{\Delta S^\circ}{R} \tag{18}$$

where change in Gibbs free energy (ΔG°), change in enthalpy (ΔH°) and change in entropy (ΔS°) are thermodynamic constants, T is the absolute temperature (K), R is the atmospheric gas constant (8.314 J/mol K) and k_c is the distribution coefficient. Here, the distribution coefficient [46] can be calculated by:

$$k_c = \frac{q_e}{C_e} \tag{19}$$

The values of ΔG°, ΔH° and ΔS° listed in the Table 4 by calculating the thermodynamic data which can be calculated by plotting $\ln k_c$ as a function of $1/T$. The positive values of ΔH° and ΔS° informs us that the biosorption process is endothermic. The negative values of ΔG° show that the biosorption process is spontaneous.

3.21. Comparison with other adsorbents

Adsorption experiments were performed using STFS for Cr(VI) removal. The adsorption capacity of Cr(VI) onto STFS was compared with different adsorbents that are reported in literature and represented in Table 5. A comparison of various adsorbents also shows that STFS has exhibited higher adsorption capacity and could be one of the best adsorbents for the removal of hexavalent chromium from aqueous solutions.

Table 5
Comparison of adsorption capacities of various adsorbents with STFS of Cr(VI) removal

Adsorbent	pH	Adsorption capacity (mg/g)	Refs.
Acacia albida	2.0	2.983	[17]
Leaves of *Euclea schimperi*	2.0	3.946	[17]
Raw *Sterculia guttata* shell	2.0	45.45	[24]
Ficus auriculata leaves powder	2.0	13.33	[36]
Sweetenia mahagoni fruit shell	3.0	2.309	[47]
Sugarcane bagasse	2.0	1.76	[48]
Peanut husk	2.0	33.11	[49]
Ficus carica	3.0	13.41	[18]
Parthenium hysterophorus weed	1.0	24.5	[23]
Erythrina variegata orientalis leaf powder	3.0	1.72	[12]
Mangrove leaf powder	2.0	60.24	[15]
Peanut shell	2.0	16.26	[50]
Wheat residue	1.0	21.34	[51]
Pineapple leaves	2.0	8.77	[52]
STFS	2.0	90.9	Present study

4. Conclusions

STFS adsorbent was collected from the NIT Calicut campus can be used as an effective biosorbent for the removal of Cr(VI) from aqueous solutions. Adsorption of Cr(VI) ions is found to be best at pH 2.0. The study also suggests that it has enough surface area and has good physical and chemical properties. The biosorption of Cr(VI) on STFS seems to be significantly affected by pH, initial Cr(VI) concentration, biosorbent size, biosorbent dosage, agitation speed and temperature. Three isotherm models seem to be best fitted with the equilibrium data from the calculated eight isotherm models. Kinetic studies reveals that Cr(VI) adsorption described results in favour of pseudo-second-order kinetic model. The Gibbs free energy calculated was negative which informs us that the adsorption process is spontaneous. The biosorption capacity of STFS was compared with other biosorbents for Cr(VI) removal and the results are listed. In overall, easy availability of this low cost STFS adsorbent seems to be an efficient one for the removal of Cr(VI).

Acknowledgements

Many thanks to Research Council for Engineering and Technology Programmes, Kerala State Council for Science, Technology and Environment, India (Grant No. ETP/02/2014/KSCSTE) for their financial support.

List of symbols

A_T — Temkin isotherm equilibrium binding constant (L/mg)
b_T — Temkin isotherm constant (J/mol)
b_L — Langmuir isotherm constant (L/mg)
C_0 — initial Cr(VI) concentration (mg/L)
C_e — Cr(VI) concentration in solution at equilibrium (mg/L)
E — mean adsorption energy (kJ/mol)
k_f — Freundlich isotherm constant $(mg/g)/(mg/L)^{1/n}$
K — coefficient related to the mean free energy of adsorption (mol^2/kJ^2)
K_j — Jovanovic isotherm constant (L/g)
M — amount of biosorbent (g)
N — adsorption intensity
Q_0 — monolayer coverage capacity (mg/g)
Q_m — maximum adsorption capacity (mg/g) in D–R model
q_{mj} — maximum adsorption capacity in Jovanovic model (mg/g)
K_H — Halsey isotherm model constant
n_H — Halsey isotherm model exponent
K_{FH} — Flory–Huggins equilibrium constant
n_{FH} — Flory–Huggins model exponent
Q — degree of surface coverage
q_e — amount of Cr(VI) ions adsorbed per unit mass of biosorbent (mg/g)
q — amount of Cr(VI) adsorbed at any time t (mg/g)
R — atmospheric gas constant (8.314 J/mol K)
R_L — separation factor
V — volume of the solution (L)
T — temperature (K)
ΔG° — Gibbs free energy (kJ/mol)
ΔH° — Enthalpy (kJ/mol)
ΔS° — Entropy (J/mol K)
k_c — distribution coefficient
R^2 — coefficient of determination
ε — Polanyi potential
k_1 — pseudo-first-order constant (min)
k_2 — pseudo-second-order constant (g/mg/min)
k_{id} — intraparticle diffusion rate constant $(mg/g/min^{1/2})$
C — intercept of intraparticle diffusion model

References

[1] B.C. Son, K.M. Park. S.H. Song, Y.J. Yoo, Selective biosorption of mixed heavy metal ions using polysaccharides, Korean J. Chem. Eng. 21(6) (2004) 1168-1172.
[2] A.E. Sikaily, A.E. Nemr, A. Khaled, O. Abdelwehab, Removal of toxic chromium from wastewater using green alga *Ulva lactuca* and its activated carbon, J. Hazard. Mater. 148 (2007) 216–228.
[3] H. Li, Z. Li, T. Liu, X. Xiao, Z. Peng, L. Deng, A novel technology for biosorption and recovery hexavalent chromium in wastewater by bio-functional magnetic beads, Bioresour. Technol. 99 (2008) 6271–6279.
[4] Website of central pollution control board. Available from: <www.cpcb.nic.in>.
[5] H. Barrera, F. Urenanunez, B. Bilyeu, C. Barreradiaz, Removal of chromium and toxic ions present in mine drainage by *Ectodermis* of *Opuntia*, J. Hazard. Mater. 136 (2006) 846–853.
[6] F. Fu, Q. Wang, Removal of heavy metal ions from wastewaters: A review, J. Environ. Manage. 92 (2011) 407–418.
[7] S. Gupta, B.V. Babu, Adsorption of chromium(VI) by a low cost adsorbent prepared from tamarind seeds, Paper presented at CHEMCON-2006, India.
[8] E.A. Oliveira, S.F. Montanher, A.D. Andrade, J.A. Nóbrega, M.C. Rollemberg, Equilibrium studies for the sorption of chromium and nickel from aqueous solutions using raw rice bran, Process Biochem. 40 (2005) 3485–3490.
[9] P. Suksabye, P. Thiravetyan, W. Nakbanpote, S. Chayabutra, Chromium removal from electroplating wastewater by coir pith, J. Hazard. Mater. 141 (2007) 637–644.
[10] J. Anandkumar, B. Mandal, Removal of Cr(VI) from aqueous solution using Bael fruit (*Aegle marmelos correa*) shell as an adsorbent, J. Hazard. Mater. 168 (2009) 633–640.

[11] Y.C. Sharma, C.H. Weng, Removal of chromium(VI) from water and wastewater by using riverbed sand: Kinetic and equilibrium studies, J. Hazard. Mater. 142 (2007) 449–454.
[12] G.V.V. Aditya, B.P. Pujitha, N.C. Babu, P. Venkateswarlu, Biosorption of chromium onto *Erythrina Variegata Orientalis* leaf powder, Korean J. Chem. Eng. 29(1) (2012) 64–71.
[13] M. Aliabadi, K. Morshedzadeh, H. Soheyli, Removal of hexavalent chromium from aqueous solution by lignocellulosic solid wastes, Int. J. Environ. Sci. Technol. 3(3) (2006) 321–325.
[14] D. Shukla, P.S. Vankar, Efficient biosorption of chromium(VI) ion by dry *Araucaria* leaves, Environ. Sci. Pollut. Res. 19 (2012) 2321–2328.
[15] T. Sathish, N.V. Vinithkumar, G. Dharani, R. Kirubagaran, Efficacy of mangrove leaf powder for bioremediation of chromium (VI) from aqueous solutions: Kinetic and thermodynamic evaluation, Appl. Water Sci. 5 (2015) 153–160.
[16] S.B. Saroj, N.D. Surendar, R.C. Gautam, R. Pradip, Adsorption of chromium(VI) by treated weed *Salvinia cucullata*, Adsorption 14 (2008) 111–121.
[17] G. Gebrehawaria, A. Hussen, V.M. Rao, Removal of hexavalent chromium from aqueous solutions using barks of *Acacia albida* and leaves of *Euclea schimperi*, Int. J. Environ. Sci. Technol. 12 (2015) 1569–1580.
[18] V.K. Gupta, D. Pathania, S. Agarwal, S. Sharma, Removal of Cr(VI) onto *Ficus carica* biosorbent from water, Environ. Sci. Pollut. Res. 20 (2013) 2632–2644.
[19] S. Arunima, G.B. Krishna, Adsorption of chromium (VI) on *Azadirachta Indica* (Neem) leaf powder, Adsorption 10 (2004) 327–338.
[20] K. Rasoul, F. Mehdi, B. Behnam, A.A. Taghizadeh, Removal of hexavalent chromium from aqueous solution by granular and powdered *Peganum Harmala*, Appl. Surf. Sci. 292 (2014) 670–677.
[21] M. Jain, V.K. Garg, K. Kadirvelu, Chromium(VI) removal from aqueous system using *Helianthus annuus* (sunflower) stem waste, J. Hazard. Mater. 162 (2009) 365–372.
[22] O.S. Amuda, F.E. Adelowo, M.O. Ologunde, Kinetics and equilibrium studies of adsorption of chromium (VI) ion from industrial wastewater using *Chrysophyllum albidum* (*Sapotaceae*) seed shells, Colloids Surf. B, Biointerfaces 68 (2009) 184–192.
[23] V. Venugopal, K. Mohanty, Biosorptive uptake of Cr (VI) from aqueous solutions by *Parthenium hysterophorus* weed: Equilibrium, kinetics and thermodynamic studies, Chem. Eng. J. 174 (2011) 151–158.
[24] S. Rangabhashiyam, N. Selvaraju, Adsorptive remediation of hexavalent chromium from synthetic wastewater by a natural and $ZnCl_2$ activated Sterculia guttata shell, J. Mol. Liquids 207 (2015) 39–49.
[25] K.Z. Elwakeel, Removal of Cr(VI) from alkaline aqueous solutions using chemically modified magnetic chitosan resins, Desalination 250 (2010) 105–112.
[26] P. Suksabye, P. Thiravetyan, Cr(VI) adsorption from electroplating plating wastewater by chemically modified coir pith, J. Environ. Manage. 102 (2012) 1–8.
[27] S. Rangabhashiyam, N. Selvaraju, Evaluation of the biosorption potential of a novel *Caryota urens* inflorescence waste biomass for the removal of hexavalent chromium from aqueous solutions, J. Taiwan Inst. Chem. Eng. 47 (2015) 59–70.
[28] K. Meghna, M. Manoj Kumar, Mass transfer and related phenomena for Cr(VI) adsorption from aqueous solutions onto *Mangifera indica* sawdust, Chem. Eng. J. 218 (2013) 138–146.
[29] A.E. Ofomaja, E.B. Naidoo, Biosorption of copper from aqueous solution by chemically activated pine cone: A kinetic study, Chem. Eng. J. 175 (2011) 260–270.
[30] A. Jamil, S. Umer, U.Z. Waheed, S. Muhammad, D. Amara, A. Shafique, Removal of Pb(II) and Cd(II) from water by adsorption on peels of banana, Bioresour Technol. 10 (2010) 1752–1755.
[31] M. Jain, V.K. Garg, K. Kadirvelu, Adsorption of hexavalent chromium from aqueous medium onto carbonaceous adsorbents prepared from waste biomass, J. Environ. Manage. 91 (2010) 949–957.
[32] J. Chen, P. Yang, D. Song, S. Yang, L. Zhou, L. Han, B. Lai, Biosorption of Cr(VI) by carbonized Eupatorium adenophorum and Buckwheat straw: Thermodynamics and mechanism Front, Environ. Sci. Eng. 8 (2014) 960–966.
[33] A. Sarı, M. Tuzen, Biosorption of total chromium from aqueous solution by red algae (*Ceramium virgatum*): Equilibrium, kinetic and thermodynamic studies, J. Hazard. Mater. 160 (2008) 349–355.
[34] A.K. Meena, G.K. Mishra, P.K. Rai, C. Rajagopal, P.N. Nagar, Removal of heavy metal ions from aqueous solutions using carbon aerogel as an adsorbent, J. Hazard. Mater. B 122 (2005) 161–170.
[35] S. Rangabhashiyam, E. Nakkeeran, N. Anu, N. Selvaraju, Biosorption potentials of a novel powder, prepared from *Ficus auriculata* leaves, for sequestration of hexavalent chromium from aqueous solutions, Res. Chem. Intermed. 41 (2015) 8405–8424.
[36] S. Rangabhashiyam, N. Anu. M.S. Giri Nandagopal, N. Selvaraju, Relevance of isotherm models in biosorption of pollutants by agricultural byproducts, J. Environ. Chem. Eng. 2 (2014) 398–414.
[37] I. Langmuir, The adsorption of gases on plane surfaces of glass, mica and platinum, J. Am. Chem. Soc. 40 (1918) 1361–1403.
[38] I.D. Mall, V.C. Srivastava, N.K. Agarwal, I.M. Mishra, Adsorptive removal of malachite green dye from aqueous solution by bagasse fly ash and activated carbon-kinetic study and equilibrium isotherm analyses, Colloids Surf. A: Physicochem. Eng. Aspects 264 (2005) 17–28.
[39] A. Nunes, A.S. Franca, L.S. Oliveira, Activated carbons from waste biomass: An alternative use for biodiesel production solid residues, Bioresour. Technol. 100 (2009) 1786–1792.
[40] D.S. Jovanovic, Physical adsorption of gases I: Isotherms for monolayer and multilayer adsorption, Colloid Polym. Sce. 235 (1969) 1203–1214.
[41] M.E. Argun, S. Dursun, C. Ozdemir, M. Karatas, Heavy metal adsorption by modified oak sawdust: Thermodynamics and kinetics, J. Hazard. Mater. 141 (2007) 77–85.
[42] W.D. Harkins, G. Jura, The decrease of free surface energy as a basis for the development of equations for adsorption isotherms and the existence of two condensed phases in films on solids, J. Chem. Phys. 12 (1944) 112–113.

[43] M. Horsfall, A.I. Spiff, Equilibrium sorption study of Al^{3+}, Co^{2+} and Ag^{2+} in aqueous solutions by fluted pumpkin waste biomass, Acta Chim. Slov. 52 (2005) 174–181.
[44] M.S. Mansour, M.E. Ossman, H.A. Farag, Removal of Cd (II) ion from waste water by adsorption onto polyaniline coated on sawdust, Desalination 272 (2011) 301–305.
[45] A.C. de Lima, R.F. Nascimento, F.F. de Sousa, J.M. Filho, A.C. Oliveira, Modified coconut shell fibers: A green and economical sorbent for the removal of anions from aqueous solutions, Chem. Eng. J. 185–186 (2012) 274–284.
[46] S. Qaiser, A.R. Saleemi, M. Umar, Biosorption of lead from aqueous solution by *Ficus religiosa* leaves: Batch and column study, J. Hazard. Mater. 166 (2009) 998–1005.
[47] S. Rangabhashiyam, N. Anu, N. Selvaraju, Equilibrium and kinetic modeling of chromium(VI) removal from aqueous solution by a novel biosorbent, Res. J. Chem. Environ. 18 (2014) 30–36.
[48] I.C. Alomá, I. Rodríguez, M. Calero, G. Blázquez, Biosorption of Cr^{6+} from aqueous solution by sugarcane bagasse, Desalin. Water Treat. 52 (2014) 5912–5922.
[49] M.T. Olguín, H.L. Gonzalez, J.S. Gomez, Hexavalent chromium removal from aqueous solutions by Fe-modified peanut husk, Water Air Soil Pollut. 224 (2013) 1654–1656.
[50] Z.A.A. Othman, R. Ali, M. Naushad, Hexavalent chromium removal from aqueous medium by activated carbon prepared from peanut shell: Adsorption kinetics, equilibrium and thermodynamic studies, Chem. Eng. J. 184 (2012) 238–247.
[51] X.S. Wang, L.F. Chen, F.Y. Li, K.L. Chen, W.Y. Wan, Y.J. Tang, Removal of Cr(VI) with wheat residue derived black carbon: Reaction mechanism and adsorption performanceJ, J. Hazard. Mater. 175 (2010) 816–822.
[52] J. Ponou, J. Kim, L.P. Wang, G. Dodbiba, T. Fujita, Sorption of Cr(VI) anions in aqueous solution using carbonized or dried pineapple leaves, Chem. Eng. J. 172 (2011) 906–913.